Proceedings of the 6th International Conference of Control, Dynamic Systems, and Robotics (CDSR'19)
Ottawa, Canada – June, 2019
Paper No. CDSR 107
DOI: 10.11159/cdsr19.107

Plasma State Control of Reactive Sputter Processes

Christian Woelfel[1], Moritz Oberberg[2], Peter Awakowicz[2], Jan Lunze[1]
[1]Institute of Automation and Computer Control / Ruhr-University Bochum
44801, Bochum, Germany
woelfel@atp.rub.de; lunze@atp.rub.de
[2]Institute for Electrical Engineering and Plasma Technology / Ruhr-University Bochum
44801, Bochum, Germany
oberberg@aept.rub.de; awakowicz@aept.rub.de

Abstract – Nonlinear reactive sputter processes are indispensable for the deposition of functional thin film layers. As the coating process is driven by a low pressure plasma the plasma state affects the thin film properties. The process behavior has specific properties. It is unstable, one specific input value can lead to different values of the plasma state and the same plasma state can be achieved by different input values. This unstable and ambiguous behavior requires a control system, which consists of a stabilizing controller, an estimation unit and a feedforward controller. In this paper, a design method for the plasma state control based of an input/output-model is proposed. Experiments show the effectiveness of the proposed control method.

Keywords**:** Process control, nonlinear systems, reactive sputter processes

1. Introduction

In today's industry thin film layers are used to enhance the properties of products like solar cells, lenses or filters. The layer deposition can be performed by reactive sputter processes. A background gas is ionized to generate a low-pressure plasma and material is sputtered from a solid target by energetic ions. The target particles are transported towards the substrate and a reactive gas is added to form a compound thin film at the substrate.

The nonlinear plasma-surface interaction plays a crucial role for process control. In particular, the same reactive gas flow can lead to different plasma states and, moreover, the same plasma state can be achieved by different values of the reactive gas flow. Depending on a specific pair of plasma state and reactive gas flow qualitatively different thin film properties can be achieved. In addition, operating points, which combine good properties of the thin film and high deposition rates, are unstable.

The control aim is to reach and to stabilize a desired operating point with the plasma state $y_{\mathrm{f}}(t)$ as controlled variable and the reactive gas flow $u(t)$ as manipulated variable. The desired plasma state $\overline{w}_{\mathrm{f}}$ and the desired process mode $\overline{w}_{\mathrm{mode}}$ serve as reference variables.

In this paper a new method for the plasma state control is proposed. Based on a discussion of the literature and the process model, the controller structure and the design method are posed. The control system (upper part of Fig. 1) consists of a feedforward controller, an estimation unit and a feedback controller to fulfill the control aim. Experiments for the controller validation show the effectiveness of the proposed design method.

2. Literature

Classical studies [1-3] on the control of reactive sputtering mainly consider secondary process variables like pressures, optical emissions or voltages to allow high-rate sputtering [4]. The authors of the present paper have provided a control-oriented process model and controller design method [5] with respect to the high-rate sputtering problem. The plasma and its properties are not directly considered by these approaches.

However, modern investigations [6-7] on the electrical properties, on the surface morphology, on the homogeneity and on the chemical composition of the thin films show the importance of the plasma density as a determining plasma state to the layer quality for different deposition processes.

The newly developed Multipole Resonance Probe [8] allows the measurement of the plasma state based on active plasma resonance spectroscopy. The sensor has been tested as a monitoring tool [9] and has been used to identify a control-oriented input/output-model of the plasma-surface process. The present paper analyzes the new model from a control-theoretic point of view to systematically design the control system.

3. Reactive Sputtering Process

3.1 Technical set-up

The experimental system is shown in Fig. 1. A gas supply provides oxygen as the reactive gas to be ionized. A mass flow controller allows the adjustment of the oxygen flow into the chamber. Its set-point is the manipulated variable $u(t)$. The pump system generates the low-pressure regime and reduces the influence of leakage fluxes from the atmosphere into the reactor. The power to ionize the gas particles is generated by a 13.56 MHz radio-frequency source. The power source operates with constant power amplitude. A matching unit decreases the reflected power from the plasma and magnets behind the target enhance the plasma density.

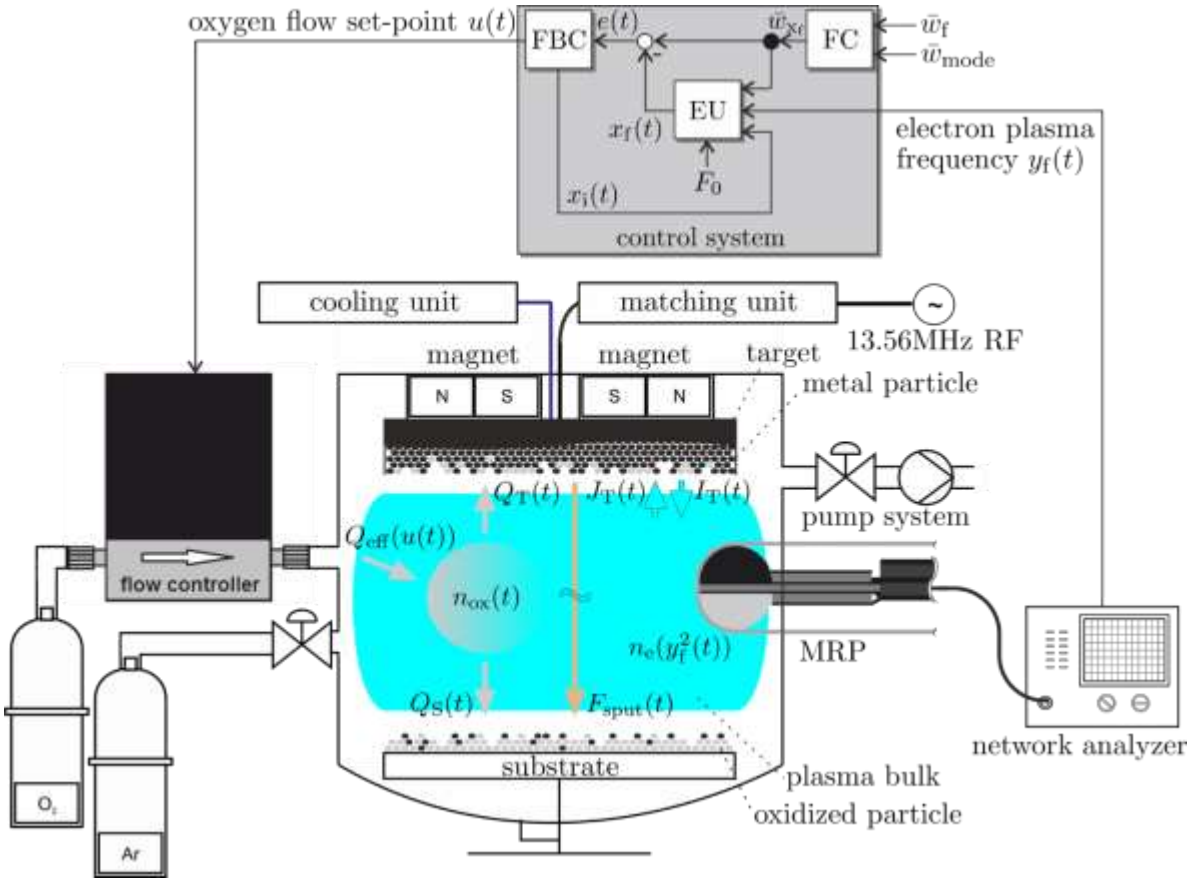

Fig. 1: Technical set-up with the closed loop consisting of a mass flow controller with the set-point $u(t)$, the Multipole Resonance Probe (MRP) and a network analyzer as sensor system to measure the electron plasma frequency y_{f}(t) and the control system with the feedforward controller (FC), the feedback controller (FBC) and the process of reactive sputter deposition (RSD). The thick arrows inside the reactor chamber represent the essential particle flows during reactive sputtering with respect to the behavior of the electron density $n_{\mathrm{e}}(t)$.

For the determination of the plasma state the sensor system is composed of the Multipole Resonance Probe and a network analyzer. The measurement principle makes use of the electron oscillation near the electron plasma frequency. An high-frequency sweep is coupled from the sensor system into the plasma, where the electrons absorb the energy and resonate. The electron density

$$n_e(t) = y_f^2(t)\frac{\varepsilon_0 m_e}{e^2} \tag{1}$$

is directly proportional to the squared electron plasma frequency $y_f^2(t)$ [10]. The remaining parameters are natural constants with ε_0 as the electrical constant, m_e as the mass of an electron and e^2 as the squared charge of an electron. In the plasma bulk the electron density is the plasma density and a controlled plasma resonance frequency implies a controlled plasma density.

3.2 Process physics

The basic physical effects during the reactive sputtering in relation to the control aim are described by the particle flows in Fig. 1. $J_T(t)$ represents the ion density, which is obtained by the acceleration of ions from the plasma bulk towards the target electrode. Contingent on the material-dependent sputter yield (ratio of sputtered particles to incoming ions) an amount $F_{sputt}(t)$ of sputtered particles are transported from the target towards the substrate. They interact with the gas particles and with the charge carriers on their way through the plasma. If they stick on the substrate surface, a thin film is built up. Aside of the heavy particle sputtering the incoming ions can also lead to an emission of electrons. This secondary electrons create a current from the target into the plasma, which is denoted by $I_T(t)$. Since the electron emission yield is depending on the material and the emitted electrons increase the electron density $n_e(t)$, the state of the surfaces is measurable by the plasma resonance frequency $y_f(t)$.

The effective flow $Q_{eff}(t)$ of oxygen into the reactor chamber is a function of the manipulated variable $u(t)$ and influences the oxygen particle density $n_{ox}(t)$. Oxygen particles can react with metallic parts of the target and with metallic parts of the substrate. Hence, the oxygen particle density is also manipulated by the accumulated oxygen particle flows $Q_T(t)$ or $Q_S(t)$ at the target and at the substrate as a function of the surface coverings. The surface covering describes the reacted surface area of the target or the substrate. In Fig. 1 the reacted particles on the electrodes are illustrated by grey dots.

Due to that plasma-surface interaction a positive feedback occurs in reactive sputtering. If the target is more and more oxidized, the amount of sputtered particles is more and more decreased, because the sputter yield for oxidized particles is lower than for metal particles. Hence, less metal particles are transported to the substrate and the surface coverage of oxidized metal is more increased. As a consequence, less oxygen particles can be removed from the reactor volume by reactions with the metallic part of the surface. An unstable process behavior occurs.

The area of this unstable operating points is the **transition zone**, which allows the high-rate deposition of stoichiometric thin films. If the process is in the stable **poisoned mode**, the surfaces are saturated with oxygen but the deposition speed is slow because of the sputter yield. Stable operating points with a low oxidization of the surfaces are referred to the **metallic mode**.

Two more modes with respect to $y_f(t)$ have to be considered because of the overlapping of two competing processes. First, the secondary electron current $I_T(t)$ and, therefore, $y_f(t)$ is increased for higher surface coverings until the surface is saturated. Second, the electron density and, therefore, $y_f(t)$ is decreased for a rise in the oxygen particle density, because more energy is consumed by the dissociation of the oxygen particles. The second effect becomes dominant for high reactive gas particle densities and it decreases the electron density and, therefore, the measured frequency. In the **surface mode** the emitted secondary electrons (first effect) from the target surface dominate the plasma state behavior and in the **collision mode** the energy transfer (second effect) in the chamber volume determines qualitatively the process.

The stable poisoned mode and a small part of the unstable transition zone belong to the collision mode. The stable metallic mode and almost all of the unstable transition zone belong to the surface mode. The modes are illustrated by Fig. 2, which shows the static process behavior. The process behavior is analyzed in Sections 3.4 and 3.5.

3.3 Mathematical model

The input/output behavior of the reactive sputter process can be described by the state equation (1) and the output equation (2). The state equation

$$\dot{x}_\mathrm{f}(t) = A_\mathrm{f} x_\mathrm{f}^3(t) + B_\mathrm{f} x_\mathrm{f}^2(t) + C_\mathrm{f} x_\mathrm{f}(t) + D_\mathrm{f} + E_\mathrm{f} u(t) \tag{1}$$

is an Abel differential equation. The output equation

$$y_\mathrm{f}(t) = -|x_\mathrm{f}(t)| + F_0 \tag{2}$$

maps the sum of the negated absolute value of the state variable $x_\mathrm{f}(t)$ and the maximum possible value F_0 of the plasma resonance frequency to the controlled variable $y_\mathrm{f}(t)$. The following parameters

$$A_\mathrm{f} = -4.03 \cdot 10^{-16},\ \ B_\mathrm{f} = -2.93 \cdot 10^{-9},\ \ C_\mathrm{f} = 0.01,\ \ D_\mathrm{f} = -7.38 \cdot 10^{5},\ \ E_\mathrm{f} = 1.17 \cdot 10^{6},\ \ F_0 = 494.00 \cdot 10^{6}$$

rounded to two decimal places, have been identified to describe the experimental system (Fig. 1).

3.4 Static behavior

In Fig. 3 the static behaviors of the state variable $\bar{x}_\mathrm{f}$ and the output variable $\bar{y}_\mathrm{f}$ in dependence upon the input variable $\bar{u}$ are shown. A single value of the input, for example $\bar{u} = 0.67$, can lead to three different values of $\bar{x}_\mathrm{f}$, which results in a S-shaped characteristic (Fig. 2, left plot). The interval $\bar{x}_\mathrm{f} \geq 0$ belongs to the collision mode (dashed line) and values $\bar{x}_\mathrm{f} \leq 0$ belong to the surface mode (solid line). The transition zone is located between the two vertexes of the static characteristics and separates the metallic mode (lower grey area) from the poisoned mode (upper grey area).

The static characteristics of the output variable $\bar{y}_\mathrm{f}$ in dependence upon the input $\bar{u}$ have the form of a loop (Fig. 2, right plot). Analogously, three values of $\bar{y}_\mathrm{f}$ can be achieved by one specific value of $\bar{u}$. However, two values of $\bar{u}$ can also lead to one specific value of $\bar{y}_\mathrm{f}$. This ambiguous behavior requires two reference values:

The desired reactive sputtering mode $\bar{w}_\mathrm{mode} \in$ {surface mode, collision mode} and the reference value $\bar{w}_\mathrm{f}$.

3.5 Dynamical behavior

The dynamical behavior is illustrated in Fig. 3. The gradient of the temporal change $\dot{x}_\mathrm{f}$ in dependence upon x_f shows that the process has one stable equilibrium state for sufficiently high or low values of the input u. For medium values of the input the process has three equilibrium states with two stable operating points and one unstable operating point. In this zone the described avalanche effect occurs and the trajectories end up in one of the two stable equilibrium points depending on the initial condition. A feedback controller is necessary to stabilize the process in the transition zone.

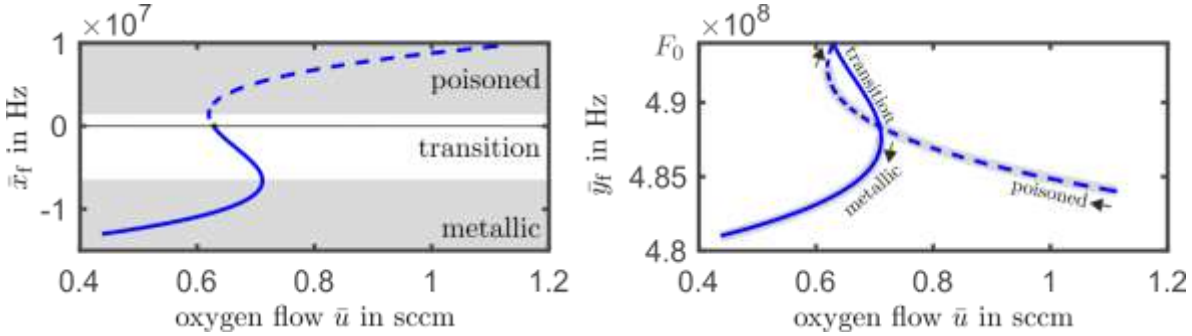

Fig. 2: Static characteristics of the state variable $\bar{x}_\mathrm{f}$ in dependence upon the oxygen flow $\bar{u}$ (left plot) and the output variable $\bar{y}_\mathrm{f}$ in dependence upon the oxygen flow $\bar{u}$ (right plot).

The dynamical characteristics for $(\dot{y}_\mathrm{f}, y_\mathrm{f})$ can be plotted (Fig. 3, right) by case distinction. For $x_\mathrm{f} \geq 0$ (collision mode) the behavior is represented by

$$\dot{y}_{\mathrm{f,c}}(t) = \dot{y}_\mathrm{f}(t) = -A_\mathrm{f}(F_0 - y_\mathrm{f}(t))^3 - B_\mathrm{f}(F_0 - y_\mathrm{f}(t))^2 - C_\mathrm{f}(F_0 - y_\mathrm{f}(t)) - D_\mathrm{f} - E_\mathrm{f}u(t). \tag{3}$$

If $x_\mathrm{f} \leq 0$ (surface mode) the output behavior is described by

$$\dot{y}_{\mathrm{f,s}}(t) = \dot{y}_\mathrm{f}(t) = A_\mathrm{f}(y_\mathrm{f}(t) - F_0)^3 + B_\mathrm{f}(y_\mathrm{f}(t) - F_0)^2 + C_\mathrm{f}(y_\mathrm{f}(t) - F_0) + D_\mathrm{f} + E_\mathrm{f}u(t). \tag{4}$$

The two process modes qualitatively determine the influence of the input by $\pm E_\mathrm{f}u(t)$. Hence, they have to be considered by the control system to establish a negative feedback and to achieve a stable closed loop.

4. Plasma State Control

4.1 Feedforward controller

The reference variables $\bar{w}_\mathrm{f}$ and $\bar{w}_\mathrm{mode}$ are mapped to

$$\bar{w}_{\mathrm{x_f}} = -\bar{w}_\mathrm{f} + F_0 \text{ for } \bar{w}_\mathrm{mode} = \text{‘collision mode’ and } \bar{w}_{\mathrm{x_f}} = \bar{w}_\mathrm{f} - F_0 \text{ for } \bar{w}_\mathrm{mode} = \text{‘surface mode} \tag{5}$$

by a feedforward controller (Fig. 1) to calculate the desired auxiliary variable $\bar{w}_{\mathrm{x_f}}$. The auxiliary variable refers to the unambiguous behavior of the state equation (1), which has a constant sign of the input. Hereby, $\bar{w}_{\mathrm{x_f}}$ can be used as a reference for the stabilizing feedback controller.

4.2 Feedback controller

The closed-loop model is expressed by

$$\begin{aligned} \dot{x}_\mathrm{f}(t) &= A_\mathrm{f}x_\mathrm{f}^3(t) + B_\mathrm{f}x_\mathrm{f}^2(t) + C_\mathrm{f}x_\mathrm{f}(t) + D_\mathrm{f} + E_\mathrm{f}u(t), \\ \dot{x}_\mathrm{i}(t) &= k_\mathrm{i}\bar{w}_{\mathrm{x_f}} - k_\mathrm{i}x_\mathrm{f}(t) \\ u(t) &= u_\mathrm{p}(t) + x_\mathrm{i}(t) = k_\mathrm{p}\bar{w}_{\mathrm{x_f}} - k_\mathrm{p}x_\mathrm{f}(t) + x_\mathrm{i}(t) \end{aligned} \tag{6}$$

with $x_\mathrm{f}(t)$ is the controlled variable, $x_\mathrm{i}(t)$ is the integrator state and $u(t)$ is the control law.

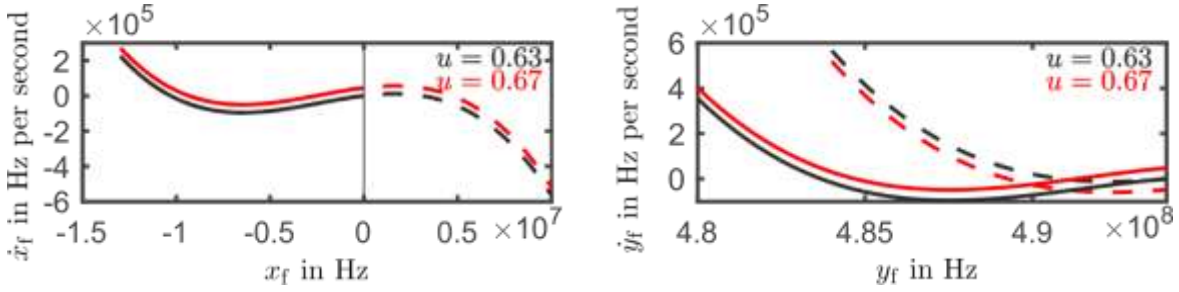

Fig. 3: Dynamical characteristics of the state variable in dependence upon x_f (left plot) and of the output variable in dependence upon y_f (right plot).

The model (6) can be transformed to

$$\dot{\tilde{x}}_{\mathrm{f}}(t) = A_{\mathrm{f}}\tilde{x}_{\mathrm{f}}^3(t) + (B_{\mathrm{f}} + 3A_{\mathrm{f}}\overline{w}_{\mathrm{x_f}})\tilde{x}_{\mathrm{f}}^2(t) + (C_{\mathrm{f}} + 3A_{\mathrm{f}}\overline{w}_{\mathrm{x_f}}^2 + 2B_{\mathrm{f}}\overline{w}_{\mathrm{x_f}} - E_{\mathrm{f}}k_{\mathrm{p}})\tilde{x}_{\mathrm{f}}(t) + E_{\mathrm{f}}\tilde{x}_{\mathrm{i}}(t) = \tilde{p}_{\mathrm{f}}(\tilde{x}_{\mathrm{f}}(t)) + E_{\mathrm{f}}\tilde{x}_{\mathrm{i}}(t),$$
$$\dot{\tilde{x}}_{\mathrm{i}}(t) = -k_{\mathrm{i}}\tilde{x}_{\mathrm{f}}(t) \tag{7}$$

by $x_{\mathrm{f}}(t) = \overline{w}_{\mathrm{x_f}} + \tilde{x}_{\mathrm{f}}(t)$ and $x_{\mathrm{i}}(t) = \tilde{x}_{\mathrm{i}}(t) - \frac{A_{\mathrm{f}}\overline{w}_{\mathrm{x_f}}^3 + B_{\mathrm{f}}\overline{w}_{\mathrm{x_f}}^2 + C_{\mathrm{f}}\overline{w}_{\mathrm{x_f}} + D_{\mathrm{f}}}{E_{\mathrm{f}}}$ (8)

to investigate the stability properties of the closed loop by application of Lyapunov's Direct Method. For this purpose, the discriminant $\Delta_{\mathrm{d}} = 4B_{\mathrm{f}}^2 - 12A_{\mathrm{f}}(C_{\mathrm{f}} - E_{\mathrm{f}}k_{\mathrm{p}})$ has to be non-positive, and, therefore the only zero of the function $\tilde{p}_{\mathrm{f}}(\tilde{x}_{\mathrm{f}}(t))$ has to be located in the origin.

By using the candidate Lyapunov function

$$V(\tilde{x}_{\mathrm{f}}, \tilde{x}_{\mathrm{i}}) = 0.5\tilde{x}_{\mathrm{f}}^2 + 0.5E_{\mathrm{f}}k_{\mathrm{i}}^{-1}\tilde{x}_{\mathrm{i}}^2, \tag{9}$$

with derivative

$$\dot{V}(\tilde{x}_{\mathrm{f}}, \tilde{x}_{\mathrm{i}}) = \tilde{x}_{\mathrm{f}}\tilde{p}_{\mathrm{f}}(\tilde{x}_{\mathrm{f}}(t)) \tag{10}$$

and by application of LaSalle's Invariance Principle it can be seen that the system is global asymptotically stable, if

$$k_{\mathrm{p}} \geq E_{\mathrm{f}}^{-1}(C_{\mathrm{f}} - B_{\mathrm{f}}^2(3A_{\mathrm{f}})^{-1}) \text{ with } E_{\mathrm{f}}^{-1} > 0 \quad \text{and} \quad k_{\mathrm{i}}E_{\mathrm{f}}^{-1} > 0 \tag{11}$$

holds.

4.3 Estimation unit

To calculate the control error $e(t) = \overline{w}_{\mathrm{x_f}} - x_{\mathrm{f}}(t)$ with respect to the reference $\overline{w}_{\mathrm{x_f}}$ the current value of the state variable $x_{\mathrm{f}}(t)$ has to be estimated. Inputs to the estimation unit are the variable $\overline{w}_{\mathrm{x_f}}$, the measured output variable $y_{\mathrm{f}}(t)$, the controller state $x_{\mathrm{i}}(t)$ and the maximum electron plasma frequency F_0. Result is the desired state variable $x_{\mathrm{f}}(t)$. Hence, the process mode (collision mode or surface mode) is automatically detected.

The estimation procedure is based on the prediction of the process behavior and the application of the process model. First, two possible values $\dot{y}_{\mathrm{f,c}}(t)$ and $\dot{y}_{\mathrm{f,s}}(t)$ of the closed-loop model (6) with respect to the case separation as in (3) and (4) have to be determined for the time T_0. For this purpose, discrete-time values $\Delta y_{\mathrm{f,c}}$ and $\Delta y_{\mathrm{f,s}}$ are calculated based on the sample time T. In the second step, the possible outputs for the time $T_1 = T_0 + T$ are predicted as

$$\hat{y}_{\mathrm{f,c}}(T_1) = \Delta y_{\mathrm{f,c}}T + y_{\mathrm{f}}(T_0) \quad \text{and} \quad \hat{y}_{\mathrm{f,s}}(T_1) = \Delta y_{\mathrm{f,s}}T + y_{\mathrm{f}}(T_0). \tag{12}$$

Third, the predicted process behaviors in terms of $\hat{y}_{\mathrm{f,c}}$ and $\hat{y}_{\mathrm{f,s}}$ are compared to the measured behavior $y_{\mathrm{f}}(T_1)$. The sign of the state variable $\hat{x}_{\mathrm{f}}$ is estimated according to

$$\begin{aligned} &\mathrm{sgn}(\hat{x}_{\mathrm{f}}) = 1 \quad \text{for } |y_{\mathrm{f}}(T_1) - \hat{y}_{\mathrm{f,c}}(T_1)| < |y_{\mathrm{f}}(T_1) - \hat{y}_{\mathrm{f,s}}(T_1)|, \\ &\mathrm{sgn}(\hat{x}_{\mathrm{f}}) = -1 \text{ for } |y_{\mathrm{f}}(T_1) - \hat{y}_{\mathrm{f,c}}(T_1)| \geq |y_{\mathrm{f}}(T_1) - \hat{y}_{\mathrm{f,s}}(T_1)| \end{aligned} \tag{13}$$

and, therefore, the value of $\hat{x}_{\mathrm{f}}$ can be calculated with (2).

The estimation process is iteratively executed during runtime. Its applicability is evaluated by experiments, which are presented in the next section.

5. Experimental Validation

In Fig. 4 the behavior of the controlled electron plasma frequency $y_f(t)$ (bottom plot) and the manipulated variable $u(t)$ (medium plot) are presented, which have been measured with the experimental set-up (Fig. 2). The controller parameters fulfill the condition (11). A stability margin has been included with respect to the estimated stabilizing $k_{p,crit} = 1.7 \cdot 10^{-8}$ and the value k_p of is set $6.0 \cdot 10^{-8}$. The remaining parameter is $k_i = 5.0 \cdot 10^{8}$.

Operating points in the collision mode are set from the start of the process to $t = 350$ seconds. This is represented by the upper plot in Fig. 4. It can be seen that the estimated variable $\hat{y}_{f,c}(t)$ is highly similar to the measured output $y_f(t)$. The state variable $x_f(t)$ follows the reference $\bar{w}_{x_f}$ as well as the controlled variable $y_f(t)$ complies with the reference $\bar{w}_f$.

At $t = 350$ seconds the desired process mode is set to the surface mode. The electron plasma frequency $y_f(t)$ is manipulated such that the maximum F_0 is crossed and the predicted value $\hat{y}_{f,s}(t)$ has a high agreement with $y_f(t)$ at $t = 380$ seconds. Set-point following is achieved at $t = 395$ seconds. In case of further step-wise set-point changes in the surface mode no substantial control error occurs.

The control system works also for switches from the surface mode to the collision mode, which can be seen at $t = 620$ seconds and $t = 1525$ seconds. In general, the process is stabilized and within the two operating modes the transient behavior of the measured variables decay rapidly. For a switch of the operating mode set-point following is achieved in less than a minute.

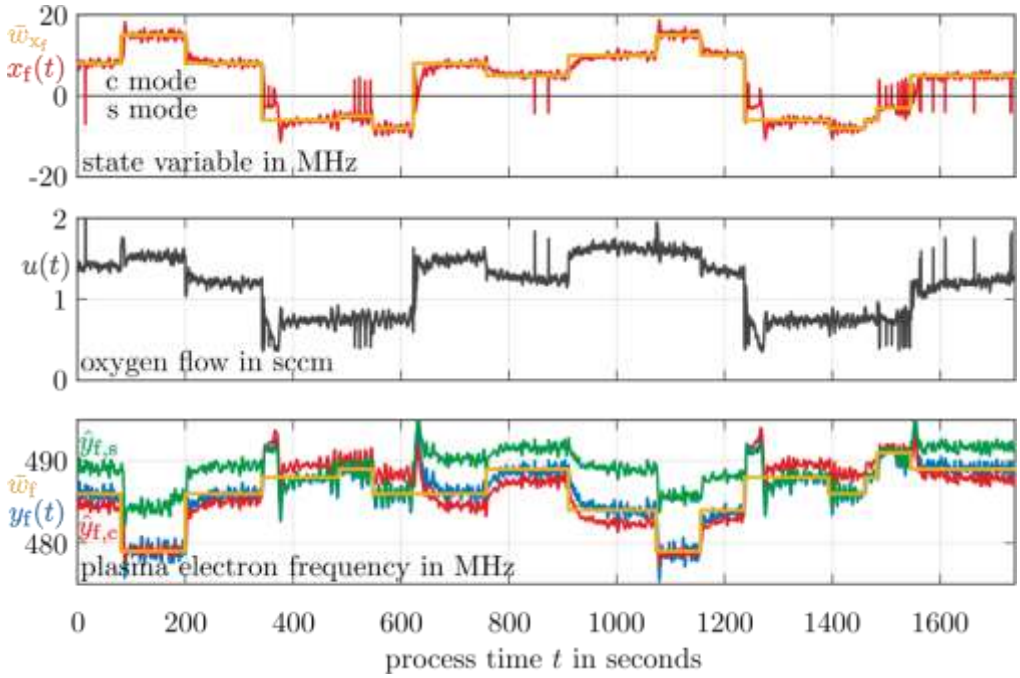

Fig. 4: Experiments on the closed loop: Behaviors of the calculated reference variable $\bar{w}_{x_f}$ and the state variable $x_f(t)$, while positive values refer to the collision (c) mode and negative values to the surface (s) mode (upper plot). Trajectory of the manipulated variable $u(t)$ (middle plot). Behaviors of the controlled variable $y_f(t)$, the reference variable $\bar{w}_f$ as well as the estimated variables $\hat{y}_{f,s}$ and $\hat{y}_{f,c}$ (lower plot).

6. Conclusion

The experimental results show that the proposed control system is able to stabilize the plasma state in reactive sputtering. A feedforward controller, an estimation unit and a feedback controller are necessary to achieve set-point following in terms of the desired sputtering mode and the desired plasma state because of the ambiguous process behavior. Future studies have to consider additional manipulated variables and controlled variables to allow a more precise of the thin film properties. For this purpose, multi-input multi-output models have to be developed.

Acknowledgements

The authors gratefully acknowledge the support providing by the German Research Foundation (DFG) within the project "Plasma-based process control of reactive sputter processes" (417888799).

The second author gratefully acknowledges the support providing by the German Federal Ministry of Education and Research (BMBF) within the project "PluTO+" (13N13212).

The third author gratefully acknowledges the support provided by the German Research Foundation (DFG) within the framework of the Transregional Collaborative Research Center SFB-TR 87 "Pulsed high power plasmas for the synthesis of nanostructured functional layers".

References

[1] W. Sproul and P. Rudnik, "Advances in partial pressure control applied to reactive sputtering," *Surface and Coatings Technology*, vol. 39-40, no. 2, pp. 499-506, 1989.

[2] S. Schiller, U. Heisig, K. Steinfelder, J. Strümpfel, R. Voigt, R. Fendler and G. Teschner, "On the investigation of d.c. plasmatron discharges by optical emission spectroscopy," *Thin Solid Films*, vol. 96, no. 3, pp. 235-240, 1982.

[3] J. Affinito and R. R. Parsons, "Mechanisms of voltage controlled, reactive, planar magnetron sputtering of Al in Ar/N_2 and Ar/O_2 atmospheres," *Journal of Vacuum Science & Technology*, vol. 2, no. 3, pp. 1275-1284, 1984.

[4] W. Sproul, D. J. Christie and D. C. Carter, "Control of reactive sputtering processes," *Thin Solid Films*, vol. 491, no. 1-2, pp. 1-17, 2005.

[5] C. Woelfel, D. Bockhorn, P. Awakowicz and J. Lunze, (in press). "Model approximation and stabilization of reactive sputter processes," *Journal of Process Control*. Available: https://doi.org/10.1016/j.jprocont.2018.06.009

[6] J. Gong, X. Zhang, Z. Pei, C. Sun and L. Wen, "Effect of enhanced plasma density on the properties of aluminium doped zinc oxide thin films produced by DC magnetron sputtering," *Journal of Materials Science & Technology*, vol. 27, no. 5, pp. 393-397, 2011.

[7] J. G. Quiñones-Galván, E. Camps, S. Muhl, M. Flores and E. Campos-González, "Influence of plasma density on the chemical composition and structural properties of pulsed laser deposited TiAlN thin films," *Physics of Plasmas*, vol. 21, no. 5, 053509, 2014.

[8] M. Lapke, J. Oberrath, T. Mussenbrock and R. P. Brinkmann, "Active plasma resonance spectroscopy: a functional analytic description," *Plasma Sources Science and Technology*, vol. 22, no. 2, pp. 1-8, 2013.

[9] T. Styrnoll, J. Harhausen, M. Lapke, R. Storch, R. P. Brinkmann, R. Foest, A. Ohl and P. Awakowicz, "Process diagnostics and monitoring using the Multipole Resonance Probe in an inhomogeneous plasma for ion-assisted deposition of optical coatings," *Plasma Sources Science and Technology*, vol. 22, no. 4, pp. 1-8, 2013.

[10] M. Lapke, T. Mussenbrock and R. P. Brinkmann, "The multipole resonance probe: A concept for simultaneous determination of plasma density, electron temperature, and collision rate in low-pressure plasmas," *Applied Physics Letter*, vol. 93, no. 5, pp. 1-3, 2008.